SIFT DESK

SDRP Journal of Nanotechnology & Material Science (ISSN: 2574-1888)

A simple and effective fluorescent and colorimetric probe for the detection of glutathione in human serum

Hai-Xia Cao[2], Yu-Sheng He[1]

DOI: 10.25177/JNMS.2.1.RA.513

Research

Received Date: 27th Apr 2019
Accepted Date: 21st May 2019
Published Date:25th May 2019

[1] School of the Environment and Safety Engineering, Jiangsu University, Zhenjiang 212013, China.

[2] School of Pharmacy, Jiangsu University, Zhenjiang 212013, China.

CITATION

Hai-Xia Cao, Yu-Sheng He, A simple and effective fluorescent and colorimetric probe for the detection of glutathione in human serum(2019)SDRP Journal of Nanotechnology & Material Science 2(1) p:83-93

ABSTRACT

Glutathione (GSH) plays fundamental roles in complicated biological systems and serves many cellular functions. Herein, a sensitive fluorescent-colorimetric dual-mode sensing platform based on carbon dots and Au nanoparticles (AuNPs) was presented for the detection of glutathione (GSH) in aqueous solution. In this system, the carbon dots (CDs) act as fluorometric reporter and the AuNPs serve a dual function as fluorescence quencher and colorimetric reporter, based on the electronic interaction. The mixture of positive charged CDs with the negative AuNPs resulted the fluorescence decreased, and color changed from red to blue. Due to the amplification effect between GSH and Au, the fluorescence intensity of CDs recovered along with the GSH concentration ranging from 0.05 to 500 μM with the detection limit of 10 nM. By monitoring the change of UV-vis spectroscopy intensity of AuNPs, the GSH could be detected with the range from 0.1 to 500 μM and a limit of detection around 0.3μM. This method was successfully applied for GSH determination in swine feeds and chicken livers. Owing to its high sensitivity, excellent selectivity and convenient procedure, this strategy will provide a promising alternative for screening.

Keywords : *Glutathione; carbon dots; gold nanoparticles; double modes; electrostatic interaction*

INTRODUCTION

Glutathione (GSH) plays fundamental roles in complicated biological systems and serves many cellular functions, which has been verified to support redox homeostasis of intracellular, signal transfer, xenobiotic metabolism and gene regulation[1-3]. It has been found that abnormal expression of GSH is closely associated with a variety of diseases, such as psoriasis, cancer, liver damage, leukocyte loss and other ailments. GSH, thus, have been function as a universal biomarker in diagnosis and therapy monitoring of cancers[4-7]. So far, efficient analytical methods for identification and quantification of GSH has been intensively investigated, including fluorescence, colorimetry, electrochemistry, surface-enhanced Raman scattering (SERS), and electrochemiluminescence[8-12]. In fact, it also must be mentioned that it is still a challenge to develop a smart GSH probe to distinguish the GSH from Hcy and Lcy. Fortunately, several findings suggested the aggregation of AuNPs can be induced by biothiols with the order of HCys > Cys > GSH, for the reason that the effects of tremendous difference in coordination capability and steric hindrance between the GSH and the competitive biothiols[13-15], then discriminate detection GSH with the AuNPs is expected, rationally.

Recently, carbon dots (CDs), as the most promising fluorescent nano materials,thanks to its distinctive properties, such as low toxicity, good compatibility, excellent solubility, low cost, and high photostability, have attracted rapidly growing interest, and discovery of carbon quantunm dots is considered as a major milestone in the development of fluorescent nanomaterials. Compared with the conventional semiconductor quantum dots (QDs), the interest in CDs research reflects the potential that they display many of the electronic and optronics properties as the same of the QDs, for instance, quantum confinement effects, while enjoying the superiority of less toxicity of being heavy matels free contained in semiconductor materials as well stability**[16-18]** have attracted rapidly growing interest, and discovery of carbon quantunm dots (CDs) is considered as a major milestone in the development of fluorescent nanomaterials. Compared with the conventional semiconductor quantum dots (QDs), the interst in CDs research reflects the potential that they display many of the electronic and optronics properties as the same of the QDs, for instance, quantum confinement effects,while enjoying the superiority of less toxicity of being heavy matels free contained in semiconductor materials as well**[19].** CDs exhibite broad UV absorption and commonly blue and green wavelengths emission and even to the red region**[20-23]**, occasionally. Carbon dots sontributed significantly to the applications of biosensors, bioimaging, drug delivery, and catalysis**[24-27]. T**here has been a sustained interest in the use of CDs for sensing application, nowadays, a series of sensitivity enhancement strategies are rapidly established and constantly remodeled for fluorescence assays, approaches widely achieved including constructing sensors via fluorescence resonance energy transfer**[28],** electron transfer process**[29],** inner filter effect (IFE)**[30],** aggregation**[31]**, and so on. Strikingly the nanosensors based on aggregation does not require any link between the receptor and the fluorophore or surface modifications of fluorescence nanomaterial, by chemical bond or physical effect directly, which provides noticeable flexbility and much more simplicity.

AuNPs, with the diameter of 1-100 nm, have become a widely applicable materials from fundamental studies to practical use in biological and chemical analysis, stimulating a large range of interest in past decades in the application of photonics, sensing, catalytic, and nanomedicine, given to their rapid and simple chemical synthesis, easy control of the narrow size distribution and shape, outstanding bio-compatibility and bio-conjugation[32-35]. As we know, AuNPs in an aqueous solution show a unique color according to their morphology and size distribution, as the results of surface plasmon resonance of noble materials. Whereas discrete AuNPs in a solution are red in color, assembled AuNPs are bluish purple in color, thus endowing AuNPs excellent properties for application, such as colorimetric or UV-spectrum. So far, various methods have been proposed to change the spectrum position according to adjust the local dielectric constant and refractive index surrounding the particles, and aggregate the nanoparticles. Specifically, the later was demonstrated in a number of colorimetric sen-

sors, since simple performce and magnificent sensitivity and selectivity[36].

The development of dual-mode sensor will make it possible to achieve detection with simple operation, high selectivity, incomparable sensitivity, and unambiguous spatiotemporal resolution, which suggests their promising applications in chemical sensing, leading many efforts paid in investigation of dual-mode sensors, in the past few years. The small molecule fluorescent probes, combined with others analytical techniques such as colorimetric method[37], mass spectrometry[38], surface enhanced raman scattering (SERS)[39, 40], high performance liquid chromatography[41], and electrochemical analysis have attracted tremendous attention. Fluorescence assays and colorimetric strategies are the classical sensing techniques for optical sensors, which can transforme molecular events into the signal of fluorescence intensity or color changes, easily, which have recently been emerged as the most talented candidates for the analytical methods for their operational simplicity, good sensitivity and low cost, addressing the deficiencies of conventional sensors.

In this work, an excellent sensitive dual-mode sensor for GSH detection with the performance of fluorescence and colorimetric was proposed, as shown in Scheme 1. Different from most of the dual-mode sensor assays, in this work, CDs with modification-free and the contrary charged resulting in a new absorption peak at 644 nm appeared by enlarged gold nanoparticles, which inducing the AuNPs color changed from red to blue and the CDs fluorescence quenching. However, the specific multidentate anchor as well with the unique steric structure existing in GSH, which shows a strong affinity to AuNPs, and renders GSH to enclose AuNPs in priority, so that, GSH can prevent the AuNPs from being aggregated and keep away from the CDs, with the results of fluorescence recovered and the absorbance at 644 nm declined. The simultaneously fluorescent and colorimetric signal events for detections of GSH provide superiority of the ultra sensitivity of fluorescent intensity and the benefit of a visual assay and exposing the potential in bioanalysis and biosensor, which was significant in disease diagnosis in the future.

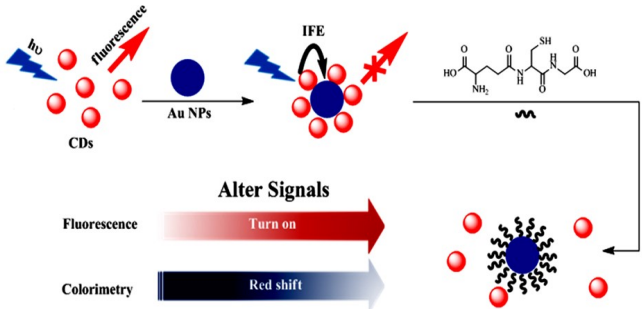

Scheme 1. Schematic illustration of the dual-modes of CDs and AuNPs for GSH detection.

MATERIALS AND METHODS

Materials and apparatus

P-phenylenediamine (p-PD), phosphoric acid, chloroauric acid ($HAuCl_4 \cdot 4H2O$), Trisodium citrate, Na_2HPO_4, NaH_2PO_4, glutathione (GSH). L-cysteine, homocysteine, methionine, threonine, tryptophan, arginine, alanine, serine, (L-Cys, Hcy, Met, Thr, Try, Arg, Ala, Ser), NaCl, KCl, $CaCl_2$, NaH_2PO_4, Na_2HPO_4 were obtained from Sinopharm Chemical Reagent Co. (China), and all chemicals were used as obtained without further purification. Human serum is from volunteers of School Hospital in Jiangsu University (Zhenjiang, Jiangsu, 212013, PR China). Ultra -pure water was prepared by a Millipore Milli-QTM system and employed throughout the following experiments.

The morphology of CDs, AuNPs were analyzed using a JEM-2100 transmission electron microscope (HRTEM, JEOL). The mean particle sizes and size distribution of the samples were analyzed using a Zeta PALS laser particle size analyzer (Brookhaven). X-ray diffraction (XRD) patterns were recorded by a D8 Advance diffractometer (Bruker). Infrared spectra were measured on a pressed KBr pellet employing a Nicolet 6700 FT-IR spectrometer (Nicolet). The fluorescence and the absorption spectra were measured with an RF-5301PC spectrofluorometer (Shimadzu) and a UV-2600 UV-Vis spectrophotometer (Shimadzu), respectively.

Synthesis of red carbon dots

A hydrothermal methodwas used to prepare the CDs. Briefly, 0.1 g p-PD and 1 mL 85% phosphoric acid were dissolved in 40 ml H2O, next the mixture was transferred into a 100 mL Telfon equipped stainless steel autoclave and heated at 180°C for 24h[42]. After cooling down to room temperature, the dark red turbid liquid was got. Then the solution were centrifuged at 13000 rpm for 10 min to remove the larger particles, and further dialyzed against deionized water for 24 h to remove the excess reactants. Under vacuum condition, the prepared CDs were then dried for 48 h at room temperatur, and finally, the carbon dots solution was stored at 4°C for further use.

Synthesis and Purification of AuNPs

Gold nanoparticles AuNPs) were reduced, in the typical way, with citrate sodium a stabiling reagent. In brief, 0.5 ml of 0.1% $HAuCl_4$ is droped into a proper amount of Ultra-pure water and heated to boiling, with stirring strongly at the same time. Then 2 ml of 1% sodium citrate are droped nto the builing solution as quickly as possible, keeping the boiling for about 30 min, and the gold nanoparticle with the color of red–purple are prepared. The solution were kept stirring until cooling down to room temperature, and the as-prepared AuNPs were stored at 4 °C for further use.

Preparation of pH buffer

To explore the optimal pH for the procedure of detection, the solutions of 0.2 M Na_2HPO_4 and 0.2 M NaH_2PO_4 were prepared for the use of buffer. We obtained the solution of different pH by the adjusting the ratio of two buffers, to correspond to the pH in real sample like human serum, we choose the range of pH from 3.90 to 8.03 to investigate.

Quantification of GSH

The ananlysis for GSH was performed in aqueous solution under room temperature, firstly. With a typical assay, standard stock solutions of GSH with various concentrations were prepared by dissolving GSH, directly, in optimal pH buffer. Afterwards, AuNPs and a certain amount of standard stock solutions were mixed under gentle shaking. Then 10 times dilution by ultrapure water of as-prepared CDs added. The record of fluorescence emission spectra during the procedure was get with excitation wavelength set at 520 nm.

To evaluate the selectivity of the nanosensor, similar amino acids including L-Cys, Hcy, Met, Thr, Try, Arg, Ala, Ser, NaCl, KCl, $CaCl_2$, NaH_2PO_4, Na_2HPO_4 was mixed with AuNPs in dissolving pH buffer firstly, and then CDs were shaked with the reaction solution gentlely. UV-vis and fluorescence spectra were recorded after CDs were mixed to the AuNPs reaction solution.

The application of GSH detection in serum samples was carried out. Previously, the real samples were centrifuged with an ultrafilter of 3000 molecular weight cutoff at 7000 rpm for 15 min and diluted 100 times by PBS. The concentration of the added GSH in serum samples was calculated using the developed sensing performce, and the recovery efficiency was carefully analyzed. In summary, all of the above samples are also measured by the UV-spectrum absorption spectrum while passing the fluorescence detection.

RESULTS AND DISCUSSION

Characterization

The morphology and structure of the as-prepared AuNPs were showed in Fig 1. As displayed in Fig 1A, the as-synthesized AuNPs were uniform in size and well monodispersed. As estimated from the typical low-magnification transmission electron microscopy (TEM) image, the diameters of AuNPs are rather small with a narrow size distribution (20±2 nm), as consistented with previous reports.

As can be seen from Fig 1B, a nanoparticle count originated from many such images, gained from different fields of the sample, verified the presence of exquisitely monodispersed, with particles in mean diameter 4.4 nm, range from 3.8-4.8 nm.

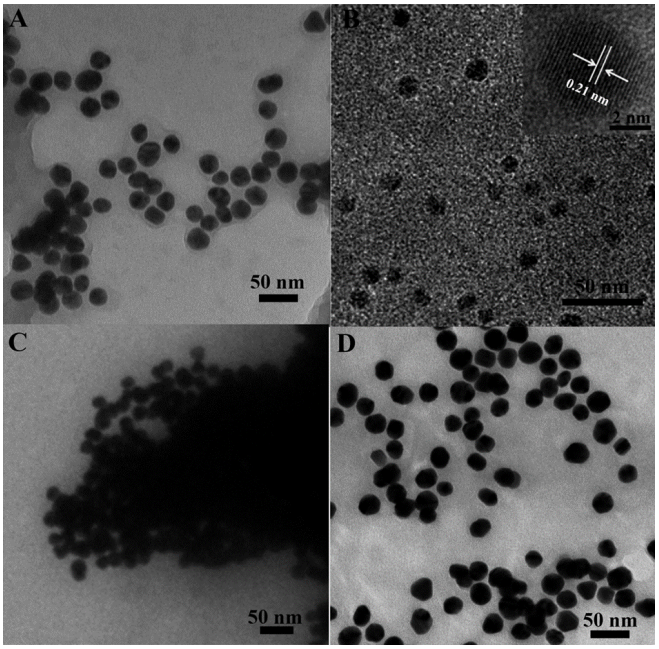

Figure 1. TEM images of (A) AuNPs; (B) CDs, inset: the HRTEM for CDs; (C) the mixture for CDs and AuNPs; (D) the AuNPs protected by GSH and then mixed with CDs.

The optical absorption peak of the gold nanoparticles was investigated, owing to the strong local field enhancement from noble metal, the AuNPs with the average size of 20 nm shows a dramatic absorption at 523 nm.While the AuNPs was mixed with CDs, an other absorption peak appeared at the wavelength of 644 nm, shown in Fig 2. The absorption peak of the CDs was noted in the UV region with an obvious absorption at 290 nm, are matched to the π-π* transitions of C=N and C=C bonds of the aromatic rings, respectively. What is more, in the visible region, a wide absorption band range in 360-600 nm can be attributed to the complex surface states of CDs. The standard signature of CDs owns a unique emission spectrum. From the principal as well as application perspective, fluorescence (FL) is one of the most engrossing behaviors of CDs. The emission peak at 602 nm with independence of the excitation wavelengths, which ranged from 440 to 550 nm, and its superlative emission intensity is noticed when the excitation wavelength is fixed at 520 nm.

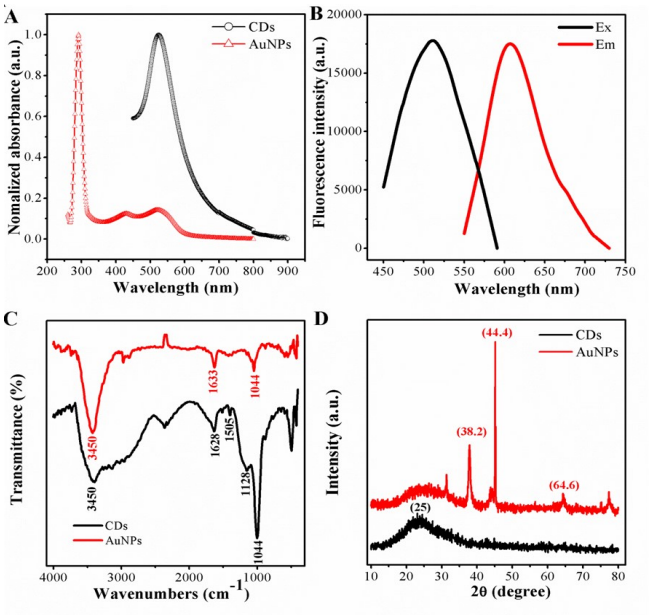

Figure 2. (A)UV-vis spectrum of AuNPs and CDs; (B) fluoresence spectrum of CDs(a)excitation and (b) emission; (C) FI-TR spectrum of AuNPs and CDs; (D) XRD pattern of AuNPs and CDs.

To further confirm, Fig 2C represents the characteristic FT-IR spectroscopy of peaks of AuNPs and CDs. First, the stabilized gold nanoparticles by sodium citrate was confirmed by FT-IR spectroscopy. The peaks of the FT-IR representing the oxygen-related groups, such as the C–O stretching peak showing at 1044 cm^{-1}, the stretching vibration peak of C=O groups at 1633 cm^{-1}, and the O–H vibration peaks at 3450 cm^{-1}. Indicating the as-prepared AuNPs were rich in carboxylic groups on the surface. The surface properties from the functional groups mean AuNPs owns a negatively charged, which matches to the Zeta potentials, the potentials of AuNPs are -1.96 mV. As for the carbon dots, the peak at 3432 cm^{-1} is due to stretching vibrations of O-H or N-H , and the strong vibration of the C-O-C appears at 1128 cm^{-1}.The peaks at 1628 cm^{-1} is caused by the stretching vibration of the C=C benzenoid ring. In additian a broad band corresponding to oxygen functionalities like -OH and C-O at 1254-1100 cm^{-1}. The sharp peak resulting from the $-NH_3^+$ shows at at 1505 cm^{-1}, indicating the positive nanoparticle CDs are preferred to accept H^+ ions in solutions. Consistently, such CDs show a zeta potential of 18.7 mV, different from those conventional negatively charged CDs, remarkably.

To gain more insight, the diffraction peaks (of AuNPs) were intense and sharp, indicating the highly crystalline features. The diffraction pattern for the negatively charged AuNPs has three peaks at 38.2, 44.4 and 64.6, corresponding to (111), (200) and (220), respectively (JCPDS No. 04-0783). The crystal phase of CDs was further verified by X-ray diffraction, as exhibited in Fig 2D. There was an obvious diffraction peak focus at about 25 which was consistent with the graphene structure of the CDs (JCPDS No. 01-0646).

The sensor mechanism

It is generally accepted that AuNPs is an excellent quench for fluorescence, containing organic fluorescent molecules, semiconductor quantum dots and carbon quantum dots, taking into account the fluorescence resonance energy transfer (FRET)[43-45]. There are relatively few studies devoted to fluorescence sensor with AuNPs by aggegation. In this script, it should be pointed out that the carbon quantum dots originated from the raw materials of P-phenylenediamine owns positive charged, may combine with AuNPs, given that electrostatic interaction happened between the two nano materials. This hypothesis was confirmed with transmission electron microscope. Furthermore, most surprisingly, the assemble morphology of CDs and AuNPs can be seen in Fig 1C .the AuNPs are aggregated compared to Fig 1A.The results are in good consistent with the observed aborsption, in Fig 3, a new peak at 644 nm appeared after mixed with CDs. On the basis of distinction in effect of coordination capability and steric hindrance as mentioned, the reaction of AuNPs with GSH can prevent the combination of gold nanoparticles with CDs. The AuNPs was incubation with GSH for a while, and mixed with as-synthesised CDs sequentially. One unanticipated finding, greatly different with the signal of mixture by CDs and AuNPs directly, was that the quenching of fluorescence by aggragation was prevented and the absorption at 644nm weaken in Fig 3, as shown in Fig 4A simultaneously. In order to trace this dynamic development, transmission electron microscope was employed again, the distribution of nanomaterials was significantly enhanced compared with Fig 1D. The results demonstrate the powerful evidence for detection of GSH in the solution of AuNPs and CDs by fluorescence and colormetics , sensitively and specifically.

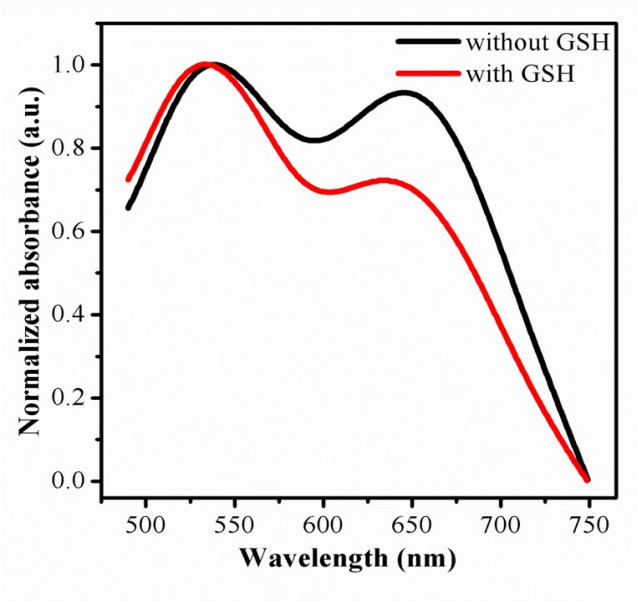

Figure 3. The changes of UV-Vis absorption of the mixture of CDs and AuNPs with and without GSH protection.

Optimization of the experimental conditions

For further development, the optimization should be studied systematically following relevant variables actors, such as dose of reactant, time and pH value and so on. The fluorescence intensity of CDs respond to the mounts of AuNPs has been discussed, since the amount of probe has a great impact on the detection sensitivity. The results show, with the mounts of AuNPs increased, the fluorescence decreased sharply until 98% roughly.

Further effort is required to understand and better control the pH for solution dominating the sensors. Contrary to expectation, the unique characteristic for stability of this sensor in a wide range of pH offers exciting opportunities to practical application, compared with traditional device. Variations in the fluorescence of the sensor were investigated over the pH from 3.90 to 8.03. Upon analysis of the intensity, less than 20% of the intensity decrease, apparently. As expected, the buffer with pH at 6.51 was exploited, for the intensity of fluorescence is is higher than the others,

Besides, to get the best recovery of the fluorescence, the time of incubation for platform was examined. The results shows, the fluorescence began to recovery once GSH added in the solution, and then kept stable, until the time exceed 2 hours. Therefore, the time for incubation was fixed at 2 hours in the further exploration.

Molecular selectivity and sensing specificity of the sensor

Owing to the good performance of the GSH selectivity detection system, the sensitivity, the linear response range, and the detection limit of the CDs and AuNPs-based fluorescence and colormitric sensing system are quantitatied with the optimum experimental conditions. As designed, firstly, the fluorescence turn-on can be the evidence for the release of CDs due to competitive binding of GSH with AuNPs As illustrated in Fig 4A, the fluorescence intensity showed different behaviors with various concentration of GSH. And the corresponding intensity increased with GSH concentration from 0.05 to 500 μM with a linear equation of $F\text{-}F_0$ = 6443.49+1997.36log*c* (*r*=0.9932).with the limited of 0.01 μM obtained, exhibited in Fig 4B. If AuNPs were firstly incubated with GSH and then mixed with CDs solution, the fluorescence would increase with the increase of GSH concentration under the light with excite with λ=365 nm, as shown in Fig 4C.

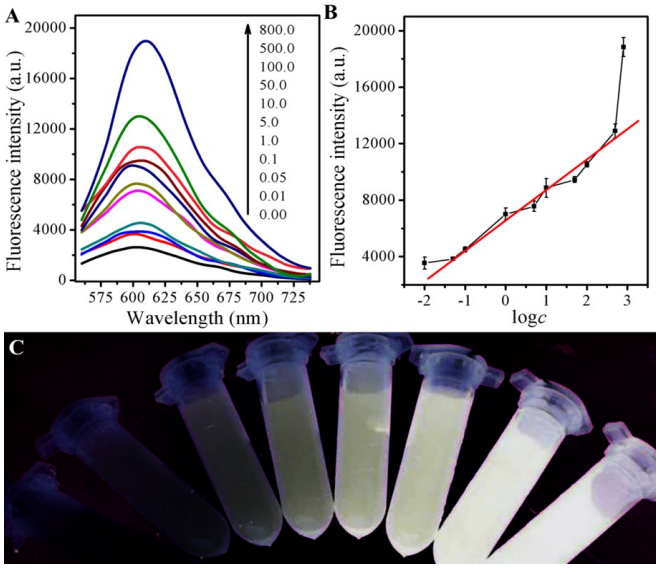

Figure 4. (A) Fluorescence spectra of the AuNPs and CDs system upon the exposure to different concentrations of GSH; (B) The link symbol of the system between $F\text{-}F_0$ and different concentrations of GSH and The linearity of the system towards different concentrations of GSH; (C) The corresponding photographs under UV lamp (λex=365 nm).

The state change for aggregation of AuNPs caused by GSH can be quantified by UV-vis spectroscopy as well. In addition to the SPR peak at 523 nm, there is another near to 644 nm, attributing to the characteristic absorption peak from the aggregation state of AuNPs. The added of GSH resulted in the systematic decline of the absorbance at 644 nm, and the absorption at 533 nm raised contrarily, shown in Fig 5A, which is supported for the color of the suspension A_{644}/A_{523}=-0.03613log*c*+0.8823 (r=0.8488) ranged from 0.1 to 30 μM, and A_{644}/A_{523}=-0.10776log*c*+0.9970 (r=0.9947) ranged from 30 to 500 μM, in Fig 5B. There is a good ratio (A_{644}/A_{523}) correlation between the absorbance at 523 nm (A_{523}) to 644 nm (A_{644}) and the color change as the result of GSH with different concentrations, ranging from 0.8-500 μM，via the following equation and a limit detection of 0.3 μM was obtained. When AuNPs were firstly incubatd with GSH and then after mixed with a CDs solution, the solution would show the color from blue to purple, and finally to red, along with the increase of GSH concentration shown in Fig 5C.

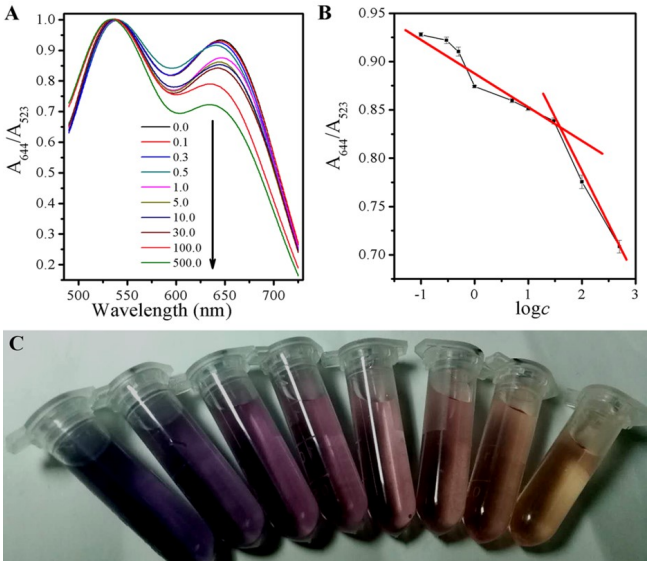

Figure 5. (A) UV-vis spectra of the AuNPs and CDs system upon the exposure to different concentrations of GSH; (B) The link symbol of the system between A644/523 and different concentrations of GSH and

The linearity of the system towards different concentrations of GSH; (C) The corresponding photographs under room light.

The selectivity of this FL and UV-vis spectra sensing system was estimated. As shown in Fig 6, besides GSH, the effects of 13 several commonly existing interfering substances, including L-Cys, Hcy, Met, Thr, Try, Arg, Ala, Ser, NaCl, KCl, $CaCl_2$, NaH_2PO_4, Na_2HPO_4 in the FL response of CDs and AuNPs were investigated. The results demonstrate these materials with 10μM have no obvious effect on the FL and colormitric as compared to 10 μM GSH, which prevented the color of system changing from red to blue gray gradually with otherwise the same conditions and keeping FL still, indicating that this assay approach possessed a ultra specificity toward GSH. To explain the observed activity, we might consider the reaction fo AuNPs and CDs changed resulted from the tremendous difference in coordination capability and steric hindrance effect.

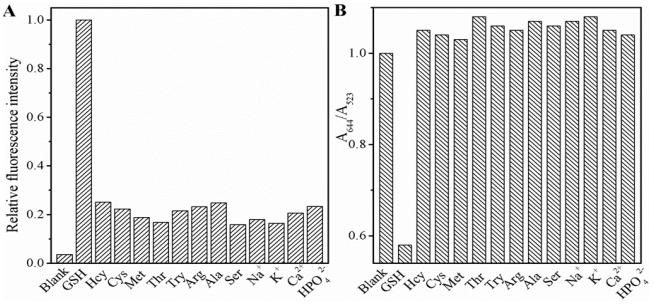

Figure 6. The selectivity of the dual modes sensor to various molecules: GSH (150 nM); other analytes (10 μM). (L-Cys, Hcy, Met, Thr, Try, Arg, Ala, Ser, NaCl, KCl, $CaCl_2$, NaH_2PO_4, Na_2HPO_4), (A) the fluorescence and (B) UV-vis spectra.

Determination of GSH in real samples

In certain complex biological samples, for instance human plasma, the concentrations of some component is abnormal, so it is necessary for potential practical assay, and the application of most common sensors is a crucial issue. To test and verify the practical application of the probes, we collected human plasma samples, diluted 100-fold with PBS (pH 7.4) before the sensing process, from local hospital. The present approach provides a linear response to GSH in spiked samples. As summarized in Table 1, the containing of GSH detected by these sensors agreed with the chose spiked values greatly. The recoveries suggested that the existence of otherwise inorganic or organic components showd no obvious affect of the detection for GSH in real samples. It reveal that the analytical performance were feasible for the practical application.

CONCLUSION

In conclusion, a simple, low cost and convenient detection method using CDs-AuNPs-based colorimetric and fluorescence probe that promises rapid, sensitive, selective detection of GSH has been developed. The results show the proposed sensor can detect GSH in concentration as low as 0.3 μM via UV-vis specture and 50 nM by fluorescence. The GSH can be distinguished with accurately, quickly and high selectivity from other existing interfering substances and the practical application for the sensors was performed with human serum samples, which supported the efficiency of the proposed probe for the determination of GSH in complicated samples, suggesting the potential in application of bioanalysis and biodection, being used in disease ananlysis and diagnosis in the future.

Table 1. Recoveries of GSH in spiked human serum samples (n = 3).

Measure mode	Found in sample (μM)	Added(μM)	Total found	Recovery	RSD
Fluorescence	0.27	0.20	0.44	94.4%	2.15%
		0.40	0.67	100.4%	1.68%
		0.60	0.85	97.5%	2.58%
Colormitric	0.46	1.00	1.54	105.5%	5.63%
		2.00	2.45	99.6%	6.06%
		3.00	3.35	96.8%	4.75%

ACKNOWLEDGEMENTS

This work was financially supported by Nature Science Foundation of Jiangsu Province (No. BK20140577), National Natural Science Foundation of China (No. 21707053) and Advanced Talents Science Foundation of Jiangsu University (10JDG038, 10JDG052).

Conflicts of interest

The authors report no conflicts of interest.

REFERENCES

[1] R. L. Krauth-Siegel, H. Bauer and R. H. Schirmers, Dithiol proteins as guardians of the intracellular redox milieu in parasites: old and new drug targets in trypanosomes and malaria-causing plasmodias, Angewandte Chemie International Edition, 44 (2005) 690-715. PMid:15657967 View Article PubMed/NCBI

[2] S. M. Kanzok, R. H. Schirmer, I. Turbachova, R. Iozef and K. Beckers, The thioredoxin system of the malaria parasite Plasmodium falciparum. Glutathione reduction revisiteds, The Journal of Biological Chemistry, 275 (2000) 40180-40186. PMid:11013257 View Article PubMed/NCBI

[3] M. Gutscher, A. L. Pauleau, L. Marty, T. Brach, G. H. Wabnitz, Y. Samstag, A. J. Meyer and T. P. Dicks, Real-time imaging of the intracellular glutathione redox potentials, Nature. Methods, 5 (2008) 553-559. PMid:18469822 View Article PubMed/NCBI

[4] S. C. Lus, Regulation of glutathione synthesiss, Molecular Aspects of Medicine, 30 (2009) 42-59. PMid:18601945 View Article PubMed/NCBI

[5] D. M. Townsend, K. D. Tew and H. Tapieros, The importance of glutathione in human diseases, Biomedicine & Pharmacotherapy, 57 (2003) 145-155. 00043-X View Article

[6] F. Kong, Z. Liang, D. Luan, X. Liu, K. Xu and B. Tangs, A Glutathione (GSH)-responsive near-infrared (NIR) theranostic prodrug for cancer therapy and imagings, Analytical Chemistry, 88 (2016) 6450-6456. PMid:27216623 View Article PubMed/NCBI

[7] S. Torres, N. Matías, A. Baulies, S. Nuñez, C. Alarcon-Vila, L. Martinez, N. Nuño, A. Fernandez, J. Caballeria, T. Levade, A. Gonzalez-Franquesa, P. Garcia-Rovés, E. Balboa, S. Zanlungo, G. Fabrías, J. Casas, C. Enrich, C. Garcia-Ruiz and J. C. Fernández-Checas, Mitochondrial GSH replenishment as a potential therapeutic approach for Niemann Pick type C diseases, Redox Biology, 11 (2017) 60-72. PMid:27888692 PMCid:PMC5123076 View Article PubMed/NCBI

[8] Q. Y. Cai, J. Li, J. Ge, L. Zhang, Y. L. Hu, Z. H. Li and L. B. Qus, A rapid fluorescence "switch-on" assay for glutathione detection by using carbon dots-MnO2 nanocompositess, Biosensors and Bioelectronics, 72 (2015) 31-36. PMid:25957074 View Article PubMed/NCBI

[9] G. Garai-Ibabe, L. Saa and V. Pavlovs, Enzymatic product-mediated stabilization of CdS quantum dots produced in situ: application for detection of reduced glutathione, NADPH, and glutathione reductase activitys, Analytical Chemistry, 85 (2013) 5542-5546. PMid:23656502 View Article PubMed/NCBI

[10] L. Y. Niu, Y. S. Guan, Y. Z. Chen, L. Z. Wu, C. H. Tung and Q. Z. Yangs, BODIPY-based ratiometric fluorescent sensor for highly selective detection of glutathione over cysteine and homocysteines, Journal of the American Chemical Society, 134 (2012) 18928-18931. PMid:23121092 View Article PubMed/NCBI

[11] W. J. Niu, R. H. Zhu, S. Cosnier, X. J. Zhang and D. Shans, Ferrocyanide-ferricyanide redox couple induced electrochemiluminescence amplification of carbon dots for ultrasensitive sensing of glutathiones, Analytical Chemistry, 87 (2015) 11150-11156. PMid:26478177 View Article PubMed/NCBI

[12] A. Saha and N. R. Janas, Detection of cellular glutathione and oxidized glutathione using magnetic-plasmonic nanocomposite-based "turn-off" surface enhanced Raman scatterings, Analytical Chemistry, 85 (2013) 9221-9228. PMid:23987745 View Article PubMed/NCBI

[13] Y. Li, P. Wu, H. Xu, H. Zhang and X. Zhongs, Anti-aggregation of gold nanoparticle-based colorimetric sensor for glutathione with excellent selectivity and sensitivitys, Analyst, 136 (2011) 196-200. PMid:20931106 View Article PubMed/NCBI

[14] F. X. Zhang, L. Han, L. B. Israel, J. G. Daras, M. M. Maye, N. K. Ly and C.-J. Zhongs, Colorimetric detection of thiol-containing amino acids using gold nanoparticless, The Analyst, 127 (2002) 462-465. PMid:12022641 View Article PubMed/NCBI

[15] N. Uehara, K. Ookubo and T. Shimizus, Colorimetric assay of glutathione based on the spontaneous disassembly of aggregated gold nanocomposites conjugated with water-soluble poly-

mers, Langmuir, 26 (2010) 6818-6825. PMid:20373784 View Article PubMed/NCBI
[16] S. N. Baker and G. A. Bakers, Luminescent carbon nanodots: emergent nanolightss, Angew. Chem. Angewandte Chemie International Edition, 49 (2010) 6726-6744. PMid:20687055 View Article PubMed/NCBI
[17] H. Li, X. He, Y. Liu, H. Huang, S. Lian, S.-T. Lee and Z. Kangs, One-step ultrasonic synthesis of water-soluble carbon nanoparticles with excellent photoluminescent propertiess, Carbon, 49 (2011) 605-609. View Article
[18] H. Li, Z. Kang, Y. Liu and S.-T. Lees, Carbon nanodots: synthesis, properties and applicationss, Journal of Materials Chemistry, 22 (2012) 24230. View Article
[19] Y. Dong, R. Wang, G. Li, C. Chen, Y. Chi and G. Chens, Polyamine-functionalized carbon quantum dots as fluorescent probes for selective and sensitive detection of copper ionss, Analytical Chemistry, 84 (2012) 6220-6224. PMid:22686413 View Article PubMed/NCBI
[20] L. Pan, S. Sun, L. Zhang, K. Jiang and H. Lins, Near-infrared emissive carbon dots for two-photon fluorescence bioimagings, Nanoscale, 8 (2016) 17350-17356. PMid:27714173 View Article PubMed/NCBI
[21] S. Sun, L. Zhang, K. Jiang, A. Wu and H. Lins, Toward high-efficient red emissive carbon dots: facile preparation, unique properties, and applications as multifunctional theranostic agentss, Chemistry of Materials, 28 (2016) 8659-8668. View Article
[22] C. Wang, K. Jiang, Q. Wu, J. Wu and C. Zhangs, Green synthesis of red-emitting carbon nanodots as a novel "turn-on" nanothermometer in living cellss, Chemistry, 22 (2016) 14475-14479. PMid:27553910 View Article PubMed/NCBI
[23] T. Zhang, J. Zhu, Y. Zhai, H. Wang, X. Bai, B. Dong, H. Wang and H. Songs, A novel mechanism for red emission carbon dots: hydrogen bond dominated molecular states emissions, Nanoscale, 9 (2017) 13042-13051. PMid:28836649 View Article PubMed/NCBI
[24] A. Zhu, Q. Qu, X. Shao, B. Kong and Y. Tians, Carbon-dot-based dual-emission nanohybrid produces a ratiometric fluorescent sensor for in vivo imaging of cellular copper ionss, Angewandte Chemie International Edition, 51 (2012) 7185-7189. PMid:22407813 View Article PubMed/NCBI
[25] C. Zhu, J. Zhai and S. Dongs, Bifunctional fluorescent carbon nanodots: green synthesis via soy milk and application as metal-free electrocatalysts for oxygen reductions, Chemical Communications, 48 (2012) 9367-9369. PMid:22911246 View Article PubMed/NCBI
[26] F. Wang, Z. Xie, H. Zhang, C.-y. Liu and Y.-g. Zhangs, Highly luminescent organosilane-functionalized carbon dotss, Advanced Functional Materials, 21 (2011) 1027-1031. View Article
[27] S. Zhu, Q. Meng, L. Wang, J. Zhang, Y. Song, H. Jin, K. Zhang, H. Sun, H. Wang and B. Yangs, Highly photoluminescent carbon dots for multicolor patterning, sensors, and bioimagings, Angewandte Chemie International Edition, 52 (2013) 3953-3957. PMid:23450679 View Article PubMed/NCBI
[28] S. H. Qaddare and A. Salimis, Amplified fluorescent sensing of DNA using luminescent carbon dots and AuNPs/GO as a sensing platform: A novel coupling of FRET and DNA hybridization for homogeneous HIV-1 gene detection at femtomolar levels, Biosensors and Bioelectronics, 89 (2017) 773-780. PMid:27816581 View Article PubMed/NCBI
[29] Q. Zhang, W. Xu, C. Han, X. Wang, Y. Wang, Z. Li, W. Wu and M. Wus, Graphene structure boosts electron transfer of dual-metal doped carbon dots in photooxidations, Carbon, 126 (2018) 128-134. View Article
[30] Q. Q. Zhang, B. B. Chen, H. Y. Zou, Y. F. Li and C. Z. Huangs, Inner filter with carbon quantum dots: A selective sensing platform for detection of hematin in human red cells, Biosensors and Bioelectronics, 100 (2018) 148-154. PMid:28886459 View Article PubMed/NCBI
[31] S. Chen, C.-H. Xu, Y.-L. Yu and J.-H. Wangs, Multichannel fluorescent sensor array for discrimination of thiols using carbon dot-metal ion pairss, Sensors and Actuators B: Chemical, 266 (2018) 553-560. View Article
[32] P. Ghosh, G. Han, M. De, C. K. Kim and V. M. Rotellos, Gold nanoparticles in delivery applicationss, Advanced Drug Delivery Reviews, 60 (2008) 1307-1315. PMid:18555555 View Article PubMed/NCBI
[33] G. Yue, S. Su, N. Li, M. Shuai, X. Lai, D. Astruc and P. Zhaos, Gold nanoparticles as sensors in the colorimetric and fluorescence detection of chemical warfare agentss, Coordination Chemistry Reviews, 311 (2016) 75-84. View Article
[34] X. Zhangs, Gold nanoparticles: recent advances in the biomedical applications, Cell Biochemistry and Biophysics, 72 (2015) 771-775. PMid:25663504 View Article PubMed/

NCBI
[35] S. Zhu, Q. Meng, L. Wang, J. Zhang, Y. Song, H. Jin, K. Zhang, H. Sun, H. Wang and B. Yangs, Highly photoluminescent carbon dots for multicolor patterning, sensors, and bioimagings, Angewandte Chemie International Edition, 52 (2013) 3953-3957. PMid:23450679 View Article PubMed/NCBI
[36] F. Chai, C. Wang, T. Wang, L. Li and Z. Sus, Colorimetric detection of Pb2+ using glutathione functionalized gold nanoparticless, ACS Appl Mater Interfaces, 2 (2010) 1466-70. PMid:20429606 View Article PubMed/NCBI
[37] Y. Shi, Y. Pan, H. Zhang, Z. Zhang, M. J. Li, C. Yi and M. Yangs, A dual-mode nanosensor based on carbon quantum dots and gold nanoparticles for discriminative detection of glutathione in human plasmas, Biosensors and Bioelectronics, 56 (2014) 39-45. PMid:24462829 View Article PubMed/NCBI
[38] M. M. Rahman, A. M. Abd El-Aty, S. W. Kim, Y. J. Lee, T. W. Na, J. S. Park, H. C. Shin and J. H. Shims, Simultaneous determination and identity confirmation of thiodicarb and its degradation product methomyl in animal-derived foodstuffs using high-performance liquid chromatography with fluorescence detection and tandem mass spectrometrys, Journal of Chromatography B,1040 (2017) 97-104. PMid:27978474 View Article PubMed/NCBI
[39] K. N. Bobba, G. Saranya, S. M. Alex, N. Velusamy, K. K. Maiti and S. Bhuniyas, SERS-active multi-channel fluorescent probe for NO: Guide to discriminate intracellular biothiolss, Sensors and Actuators B, 260 (2018) 165-173. View Article
[40] D. Li, Y. Ma, H. Duan, W. Deng and D. Lis, Griess reaction-based paper strip for colorimetric/fluorescent/SERS triple sensing of nitrites, Biosensors and Bioelectronics, 99 (2018) 389-398. PMid:28806669 View Article PubMed/NCBI
[41] H. Chen, L. Jin, Q. Chang, T. Peng, X. Hu, C. Fan, G. Pang, M. Lu and W. Wang, Discrimination of botanical origins for Chinese honey according to free amino acids content by high-performance liquid chromatography with fluorescence detection with chemometric approachess, Journal of the Science of Food and Agriculture, 97 (2017) 2042-2049. PMid:27558519 View Article PubMed/NCBI
[42] J. Chen, J. S. Wei, P. Zhang, X. Q. Niu, W. Zhao, Z. Y. Zhu, H. Ding and H. M. Xiongs, Red-emissive carbon dots for fingerprints detection by spray method: coffee ring effect and unquenched fluorescence in drying processs, ACS Applied Materials & Interfaces, 9 (2017) 18429-18433. PMid:28537370 View Article PubMed/NCBI
[43] A. Samanta, Y. Zhou, S. Zou, H. Yan and Y. Lius, Fluorescence quenching of quantum dots by gold nanoparticles: a potential long range spectroscopic rulers, Nano Letters, 14 (2014) 5052-5057. PMid:25084363 View Article PubMed/NCBI
[44] Y. Yang, J. Huang, X. Yang, K. Quan, H. Wang, L. Ying, N. Xie, M. Ou and K. Wangs, FRET nanoflares for intracellular mRNA detection: avoiding false positive signals and minimizing effects of system fluctuationss, Journal of the American Chemical Society, 137 (2015) 8340-8343. PMid:26110466 View Article PubMed/NCBI
[45] A. D. Quach, G. Crivat, M. A. Tarr and Z. Rosenzweigs, Gold nanoparticle-quantum dot-polystyrene microspheres as fluorescence resonance energy transfer probes for bioassayss, Journal of the American Chemical Society, 133 (2011) 2028-2030. PMid:21280652 View Article PubMed/NCBI